

Mid-Infrared Spectra of Radio Galaxies and Quasars

P. M. Ogle

Spitzer Science Center, Caltech, 220-6, Pasadena, CA 91125

R. R. J. Antonucci

Physics Department, University of California, Santa Barbara, CA 93106

D. Whysong

*NRAO, Array Operations Center, P.O. Box O, 1003 Lopezville Road,
Socorro, NM 87801-0387*

Abstract. *Spitzer* Infrared Spectrograph (IRS) observations of 3C radio galaxies and quasars shed new light on the nature of the central engines of AGN. Emission from silicate dust obscuring the central engine can be used to estimate the bolometric luminosity of an AGN. Emission lines from ions such as O IV and Ne V give another indication of the presence or lack of a hidden source of far-UV photons in the nucleus. Radio-loud AGN with relative-to-Eddington luminosity ratios of $L/L_{\text{Edd}} < 3 \times 10^{-3}$ do not appear to have broad optical emission lines, though some do have strong silicate emission. Aromatic emission features from star formation activity are common in low-luminosity radio galaxies. Strong H₂ pure-rotational emission lines are also seen in some mid-IR-weak radio galaxies, caused by either merger shocks or jet shocks in the interstellar medium.

1. Mid-IR Spectra

We report on *Spitzer* IRS spectrophotometry of 72 3C radio galaxies and quasars. Our survey of a complete [redshift $z < 1.0$ and $S_{\nu}(178 \text{ MHz}) > 16.4 \text{ Jy}$] sample of 52 Fanaroff and Riley (FR) type II (edge-brightened) radio galaxies and quasars has been published (Ogle, Whysong, & Antonucci 2006). We are conducting a complementary survey of 20 lower luminosity ($z < 0.1$) FR I radio galaxies to determine the nature of their central engines. Low-resolution spectra of FR I radio galaxies were taken with an exposure time of 480–1440 s per spectral order. Radio galaxies show a wide variety of mid-IR spectral features and can be classified by the strength of those features (Fig. 1).

Broad-line radio galaxies (and quasars) such as 3C 120 are characterized by high-ionization emission lines, including [O IV], [Ne V], [S IV] and [Ne VI], and strong silicate dust emission bumps at 10 and 18 μm . The high-ionization lines are powered by far-UV photons from a luminous accretion disk. The silicate emission is produced by dust out of the line-of-sight that absorbs a large fraction ($\sim 20\%$) of the luminosity from the accretion disk. Though 3C 120 has a relativistic radio jet viewed at a small angle ($< 20^\circ$), the mid-IR spectrum does not appear to contain a large fraction of synchrotron emission. In contrast, the

spectrum of BL Lac is a pure power law, presumably dominated by synchrotron emission from its relativistically beamed jet.

Mid-IR-weak radio galaxies such as NGC 6251 and 3C 270 have low-ionization emission line spectra from [Ne III], [Ne II], and [Ar II]. There is no strong source of UV photons from the nuclei to power higher-ionization lines such as [Ne V] (at least at a detectable level). Curiously, however, there are strong silicate emission features that dominate the mid-IR continuum. Perhaps the AGN continuum is powerful enough to warm circumnuclear dust, even though it is not powerful enough to produce high-ionization lines or a broad-line region.

In some sources, such as 3C 31 and 3C 293, large-equivalent width aromatic features from polycyclic aromatic hydrocarbons (PAHs) indicate a large starburst fraction. Any AGN contributions to the spectra are difficult to measure because they are significantly weaker than the starbursts. PAH features (especially at $11.3\ \mu\text{m}$) are also visible at lower equivalent width in most other radio galaxies (except BL Lac). Evidently, the radio galaxy hosts are not dead ellipticals but instead contain a rich ISM capable of forming new stars.

2. AGN Luminosities

Mid-IR spectroscopy is a powerful way to estimate the bolometric luminosities of AGNs, unhampered by extinction effects (; Ogle et al. 2006). The ratio of mid/far-IR emission from 3C quasars and radio galaxies varies by less than a factor of 3 (Shi et al. 2005), indicating very little mid-IR absorption or anisotropy. However, a plot of $\nu L_\nu(15\ \mu\text{m})$ vs. $\nu L_\nu(178\ \text{MHz})$ shows a range of 3 orders of magnitude in mid-IR luminosity for a given radio luminosity (Fig. 2). Radio jet power is not tightly correlated with accretion disk luminosity, so some other parameter such as black hole spin may be important for driving radio jets.

Considering first the FR II narrow-line radio galaxies (NLRGs) in Fig. 2, we see that only 50% have mid-IR luminosities comparable to quasars and broad-line radio galaxies [$\nu L_\nu(15\ \mu\text{m}) > 10^{44}\ \text{ergs s}^{-1}$]. The rest are mid-IR-weak, even though they have powerful radio jets (Ogle et al. 2006). Mid-IR-weak FR IIs are a factor of ~ 10 brighter in the mid-IR than the average FR I radio galaxy, and may be considered higher-luminosity cousins to FR Is.

Most of the FR I radio galaxies in our sample (except 3C 120 and Per A) are mid-IR-weak and have no broad emission lines (Fig. 2). Several authors have suggested that FR I jets are powered by extremely sub-Eddington, radiatively inefficient accretion flows (Reynolds et al. 1996). To test this hypothesis, we estimate the mass of the central supermassive black hole from the host K -band stellar luminosity and use this together with the IR luminosity to estimate the Eddington ratio. We find that all mid-IR-weak FR Is (and FR IIs) have $L/L_{\text{Edd}} < 3 \times 10^{-3}$, and no broad emission lines in their optical spectra, consistent with the absence of a luminous, optically thin accretion disk.

3. H₂ Emission

Roughly 20% of the mid-IR-weak radio galaxies have very large equivalent width H₂ emission lines in their spectra (e.g., 3C 293, Fig. 1). In contrast, very few mid-IR luminous radio galaxies have detectable H₂ emission (e.g., Per A and 3C 433), and the lines have low equivalent width. We suggest that the H₂ emission is therefore *not* powered by X-rays from the AGN.

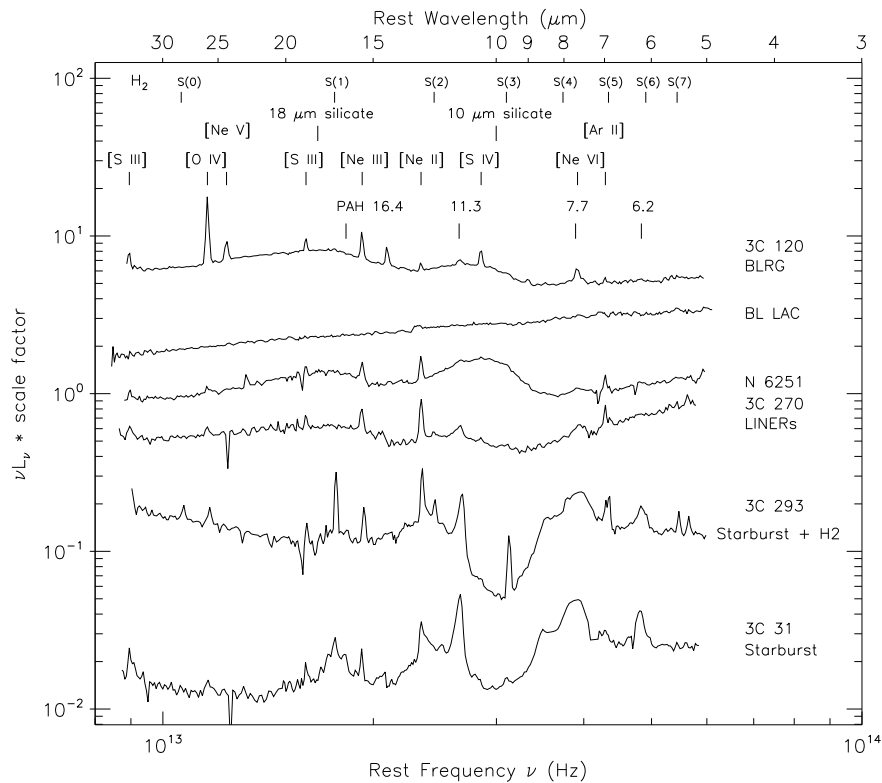


Figure 1. *Spitzer* IRS spectra of radio galaxies. Sources range from AGN-dominated at the top to starburst-dominated at the bottom. High-ionization lines are excited by far-UV continuum from the accretion disk in 3C 120. BL Lac has a power-law synchrotron emission spectrum. LINER galaxies NGC 6251 and 3C 270 have strong silicate emission features at 10 and 18 μm . Very strong H_2 lines are seen from 3C 293. Polycyclic aromatic hydrocarbon features from star formation activity dominate the spectrum of 3C 31.

The galaxy 3C 293 is the brightest example of a radio galaxy with strong H_2 emission. An excitation diagram of the H_2 pure rotational levels indicates a range of gas temperature from 300–1400 K. The luminosity of the mid-IR H_2 lines sums to 6.0×10^{41} ergs s^{-1} , from a warm molecular hydrogen mass of $3 \times 10^8 M_\odot$. Radio observations of CO emission indicate roughly $2 \times 10^{10} M_\odot$ of cold molecular hydrogen in 3C 293 (Evans et al. 1999). The host galaxy is very dusty and has a distorted morphology indicating a recent interaction with another galaxy. In addition, high-velocity H I absorption and N II emission (Morganti et al. 2003; Emonts et al. 2005) indicate a strong interaction between the radio jet and host galaxy ISM.

Because of the rich phenomenology of H_2 -emitting radio galaxies, it has proven difficult to determine the primary power source. It is likely that H_2 is thermally excited in slow (non-radiative) shocks in the ISM. These shocks could be from molecular gas accretion from companions or the IGM, or jet shocks. We

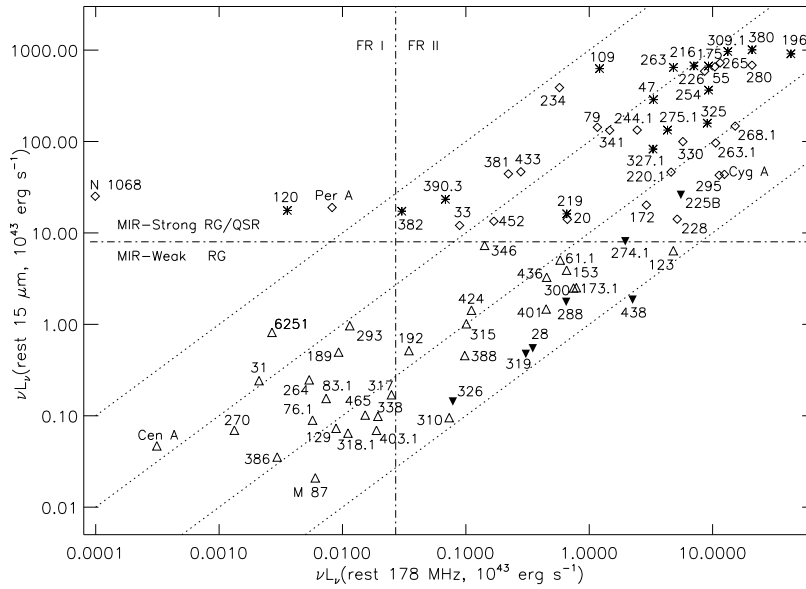


Figure 2. Mid-IR luminosity at 15 μm vs. radio luminosity at 178 MHz. Quasars (asterisks) and obscured type 2 quasars (diamonds) have $\nu L_\nu(15\mu\text{m}) > 10^{44}$ ergs s^{-1} . Mid-IR-weak FR IIs and FR Is (triangles, filled = upper limit) have lower luminosities and none of them have broad emission lines. For comparison, the Seyfert 2 galaxy NGC 1068 is also shown.

are pursuing narrow-band imaging and spectroscopy of near-IR H_2 ro-vibrational lines to isolate the power source.

Acknowledgments. This work is based on observations made with the *Spitzer* Space Telescope, operated by the Jet Propulsion Laboratory, California Institute of Technology under NASA contract 1407. Support for this research was provided by NASA through an award issued by JPL/Caltech.

References

- Emonts, B. H. C., Morganti, R., Tadhunter, C. N., Osterloo, T. A., Holt, J., & van der Hulst, J. M. 2005, *MNRAS*, 362, 931
- Evans, A. S., Sanders, D. B., Surace, J. A., & Mazzarella, J. M. 1999, *ApJ*, 511, 730
- Morganti, R., Osterloo, T. A., Emonts, B. H. C., van der Hulst, J. M., & Tadhunter, C. N. 2003, *ApJ*, 593, L69.
- Ogle, P., Whysong, D., & Antonucci, R. 2006, *ApJ*, 647, 161
- Reynolds, C. S., Di Matteo, T., Fabian, A. C., Hwang, U., & Canizares, C. R. 1996, *MNRAS*, 283, L11
- Shi, Y., et al. 2005, *ApJ*, 629, 88
- Whysong, D. H., & Antonucci, R. R. J. 2004, *ApJ*, 602, 116